High-Resolution ESR Study of the H···CH_3, H···CHD_2, D···CH_2D, and D···CD_3 Radical Pairs in Solid Argon

Kenji Komaguchi,* Kotaro Nomura, and Masaru Shiotani*

Department of Applied Chemistry, Graduate School of Engineering, Hiroshima University, Higashi-Hiroshima 739-8527, Japan

Received: June 15, 2006; In Final Form: October 20, 2006

High-resolution electron spin resonance (ESR) spectra of radical pairs of a hydrogen atom that coupled with a methyl radical (H···CH_3, H···CHD_2, D···CH_2D, and D···CD_3) were observed for X-ray irradiated solid argon containing selectively deuterium-labeled methanes, CH_4, CH_2D_2, and CD_4, at 4.2 K. The double-quartet ^{1}H-hyperfine (hf) splittings of ca. 26 and 1.16 mT at the $\Delta m_s = \pm 1$ and $\Delta m_s = \pm 2$ transitions, which are one-half of the isotropic ^{1}H-hf splittings of an isolated H-atom and a CH_3 radical, were attributed to the H···CH_3 pair. The ^{1}H-hf splittings at the $\Delta m_s = \pm 1$ transition were further split by the fine structure (fs) due to the electron dipole−dipole coupling. Because of the high-resolution spectra, three different sets of the fs splitting, d, are clearly resolved in the spectra of both the H···CH_3 and the D···CD_3 pairs. The separation distance (inter-spin distance), R, between the H-atom and the CH_3 radical being in pairs was evaluated from the d values based on a point−dipole interaction model. For the case of the H···CH_3 pair, the observed d values of 4.2, 4.9, and 5.1 mT yield the respective separations, $R = 0.87$, 0.83, and 0.82 nm, to probe the trapping site of the pair in an Ar crystalline lattice (fcc). For the pair with $R = 0.87$ nm, for example, we propose that the CH_3 radical occupies a substitutional site and the counter H-atom occupies either the interstitial tetrahedral sites directed away from the CH_3 radicals by a distance of 0.87 nm or the interstitial octahedral sites by a distance of 0.88 nm. When a mixture of CH_4 and CD_4 in a solid Ar matrix was irradiated, only two different radical pairs, H···CH_3 and D···CD_3, were observed. This result clearly demonstrates that the hydrogen atom and methyl radicals, which undergo a pairwise trapping, can originate from the same methane molecule.

1. Introduction

The triplet state radical pairs of small organic molecules have attracted much attention and have been extensively studied by electron spin resonance (ESR) spectroscopy,[1−11] due to their importance as primary unstable species in chemical reactions, especially in radiation chemistry and photochemistry. The radical pairs are characterized by weak signals at the forbidden $\Delta m_s = \pm 2$ transition ($g \approx 4$), and a fine structure (fs) due to the electron dipole−dipole interaction (zero-field splitting) at the allowed $\Delta m_s = \pm 1$ transition ($g \approx 2$) in cw-ESR. The ESR parameters such as hyperfine (hf) structure and fs can potentially provide detailed information about the orientation and trapping sites of radical pairs as well as their inter-spin distance and electronic structures.

Gordy et al.[5] first reported the ESR spectrum of the triplet state radical pair of the H-atom coupled with the CH_3 radical, H···CH_3, formed in γ-irradiated solid methane at 4.2 K. The spectrum was analyzed in terms of an axially symmetric fs with a d parameter of 9.1 mT. The d value of 9.1 mT corresponds to an inter-spin (separation) distance of $R = 0.68$ nm, suggesting that the H-atom and the CH_3 radical can be located on opposite sides of one CH_4 molecule. Next, Toriyama et al.[6] confirmed the experimental result by Gordy et al. and further examined the spatial distribution of H···CH_3 radical pairs with different inter-spin distances in an X-ray irradiated solid methane based on a line shape analysis of the H-atom absorption at $\Delta m_s = \pm 1$. In their analysis, however, the inter-spin distances greater than 0.68 nm may not be accurate, because the spectral line width was broadened, probably with unresolved super-hf splittings due to the protons of the surrounding methane molecules, and any fs patterns except for that with $d = 9.1$ mT were not resolved.

The rare-gas matrix isolation method has been developed to observe a high-resolution ESR spectrum for unstable intermediate radicals from solute molecules/atoms.[7−10,12−17] Knight et al. carried out the ESR studies of radicals generated in neon matrices containing methanes by several independent methods including photoionization, electron bombardment, x-irradiation, and pulsed-laser surface ionization technique.[13,15,16] By employing any method, the CH_4^+ radical cation was generated as a major paramagnetic species; CH_3 radical and H_2O^+ (impurity) radical cation were minor species. No ESR spectra due to the H···CH_3 radical pairs were observed in the neon matrices. Instead, when smaller molecules such as H_2 and N_2 were employed as a solute, the ESR spectra characteristic of H···H pairs were clearly observed in solid Ne, Ar, Kr, and Xe matrices, and N···N radical pairs in a solid Ne matrix.[7,9,10] The ESR resolution of the radical pairs was considerably improved by the rare-gas matrix technique, which enabled one to discuss the spectral line shape in terms of electronic state mixing effects. For the H···H pairs, however, any fs patterns at $\Delta m_s = \pm 1$ could not be observed. On the other hand, Van Zee et al.[8] observed the ESR spectra of H···NH_2 and D···ND_2 radical pairs in solid Ar and Kr matrices at both $\Delta m_s = \pm 1$ and $\Delta m_s = \pm 2$ bands, but it was difficult to assign definitely the lines at the $\Delta m_s = \pm 1$ band to the same radical pair observed at the

* Corresponding authors. Tel.: +81-82-4247737. Fax: +81-82-4245494. E-mail: K.K., okoma@hiroshima-u.ac.jp; M.S., mshiota@hiroshima-u.ac.jp.

10.1021/jp063723z CCC: $37.00
Published on Web 01/04/2007

$\Delta m_s = \pm 2$ band. Thus, even using the rare-gas matrix isolation technique, it is often difficult to observe the same radical pair at both the $\Delta m_s = \pm 1$ and the $\Delta m_s = \pm 2$ bands. The difficulty may arise from a variety of inter-spin distances of the pair in the solid matrix and/or interference by intense signals from other radicals at the $\Delta m_s = \pm 1$ band.[7−9] To examine the electronic structure of the radical pairs and their spatial distribution in detail, the high-resolution observation and accurate assignment of both $\Delta m_s = \pm 1$ and ± 2 bands are required.

In our previous paper,[18] we reported the high-resolution ESR spectra of a series of selectively D-labeled methyl radicals isolated in a solid Ar matrix at 4 K. The methane molecule and Ar atom have almost the same van der Waals diameter with a spherical form.[19] This unique combination of methane as the solute and Ar as the matrix possibly leads to a homogeneous solid mixture by rapid quenching at the low temperature of 4 K. This methodology combined with 4 K X-ray irradiation could successfully overcome the above-mentioned difficulties in observing the radical pairs. We now report the highly resolved ESR spectra of the spin exchanged radical pairs of the hydrogen atom coupled with the methyl radical, H···CH_3, H···CHD_2, D···CH_2D, and D···CD_3, which were generated and trapped in an X-ray irradiated solid Ar matrix containing a small amount of methanes. When the ESR spectra of the CH_4/Ar sample the same as in the previous study[18] were recorded under the conditions of higher microwave powers and amplitude gains, new ESR spectra attributable to the H···CH_3 radical pairs were clearly observed at both the allowed $\Delta m_s = \pm 1$ and the forbidden $\Delta m_s = \pm 2$ transitions in addition to the isolated H-atoms, CH_3 radicals, and CH_4^+ radical cations. The observed high-resolution spectra allowed us to determine the accurate ESR hf and fs parameters. The ESR studies of the irradiated CH_4-CD_4 mixture/Ar and CH_2D_2/Ar systems were also carried out. On the basis of the experimental results, we discuss the inter-spin distance and the trapping sites of the H···CH_3 radical pairs and their formation reactions in the irradiated solid Ar matrix at 4 K.

2. Experimental Section

The chemicals used in this study were Ar (a purity of more than 99.9999%, Nippon Sanso Corp.), CH_4 (a purity of 99.97%, Takachiho Trading Co., Ltd.), CH_2D_2 (>98 atom % D, ISOTEC INC.), and CD_4 (99 atom % D, ICON). The gas samples of Ar containing 0.01−0.5 mol % of either CH_4, CH_2D_2, or CD_4 were prepared and transferred to a glass vessel (inner volume of 250 cm^3) connected with a Suprasil ESR sample tube (4 mm o.d.) up to a pressure of 300 Torr on a vacuum line operated by an oil diffusion pump. An Ar sample containing an equimolar mixture of CH_4 with CD_4 (0.25 mol % each) was also prepared. We modified a cryostat (Oxford, ESR 900) to irradiate the sample with X-ray and make ESR measurements successively at 4 K. The tip part of the ESR tube was rapidly cooled to 4 K to condense the gas mixture and subjected to X-ray irradiation (target: W, 50 kV−45 mA) to a dose of ca. 0.2 kGy. The ESR spectra were recorded using a Bruker ESP300E spectrometer at the microwave power of 0.2 μW−6.3 mW in the temperature range of 4−25 K. The microwave frequency and magnetic field were calibrated using a microwave frequency counter 5350B (Hewlett-Packard) and an NMR gauss meter ER035M (Bruker), respectively. The spectral line shapes were simulated using the program SinFonia (ver. 1.25), supplied by Bruker.

3. Results and Discussion

3.1. Isolated Methyl Radicals. In a previous paper, we reported the high-resolution ESR spectra of a series of deuterium labeled methyl radicals, CH_3, CD_3, CH_2D, and CHD_2, isolated in a solid Ar matrix.[18] The present ESR study of the radical pairs is an extension of the previous one. We now briefly summarize the results of the methyl radicals for the readers to easily understand the present topics.

The X-ray irradiated CH_4/Ar sample gave a quartet ESR spectrum with an equal-intensity and an isotropic H-hf splitting of 2.315 mT below 6 K and was attributed to the A_1-lines ($m_I = \pm 1/2, \pm 3/2$) in the D_3 symmetry of the isolated CH_3 radical; m_I stands for the z-component of the total nuclear spin state of the three hydrogen nuclei involved. The spectral resolution was very high with a line width of 0.007 mT, so that the hf lines due to the D-atom in the CH_2D radical as well as the ^{13}C atom in the $^{13}CH_3$ radical were clearly observed in their natural abundance of 1.1% (^{13}C) and 0.015% (D) at 20 K, respectively. Upon increasing the temperature above 12 K, a new doublet, E-lines, with the same separation as the A_1-line, appeared and increased in intensity with the increasing temperature, but of which positions are 0.024 mT higher than the inner two A_1-lines ($m_I = \pm 1/2$). The temperature dependence of the spectra was successfully explained in terms of nuclear spin-rotation couplings using a three-dimensional free quantum-rotor model. That is, applying the Pauli principle the A_1-lines with the 1:1:1:1 quartet of the CH_3 radical was attributed to the four totally symmetric A_1 nuclear spin states coupled with the rotational ground state, $J = 0$, in D_3 symmetry.[11,18] On the other hand, the E-lines were attributed to the nuclear spin states coupled with the $J = 1$ rotational state.[11,18] Furthermore, the interesting abnormal intensities observed for the D-labeled methyl radicals, CH_2D, CHD_2, and CD_3, and their temperature dependences were fully analyzed by the nuclear spin-rotation couplings.[18]

3.2. H···CH_3 Radical Pairs Formed in the Irradiated CH_4/Ar System. *3.2.1. Spectra at $\Delta m_s = \pm 2$ Transition.* Figure 1a shows the ESR spectrum at the $\Delta m_s = \pm 2$ transition observed at 4 K for a CH_4 (0.05 mol %)/Ar sample immediately after X-ray irradiation. The spectrum consists of at least three different sets of lines. They are a doublet with a splitting of ca. 26 mT accompanied by a multiplet (species "A"), a broad singlet centered at ca. 159 mT (species "B"), and a poorly resolved weak multiplet at ca. 169 mT (species "C"). The most noticeable lines here are from species A. Species B is an unidentified radical species. Species C consists of a multiplet with ca. 1 mT separation and may be attributable to a CH_3 radical coupled with another CH_3 radical, that is, CH_3···CH_3 radical pairs.[6] We do not go into further details about the latter two species, B and C, in the present paper.

Species A has a slightly complicated spectrum. By annealing the sample at a different temperature, the spectrum was successfully analyzed in terms of three different sets of double quartets, as seen in Figure 1b−d. The double quartet lines at 5.8 K marked by "open triangle" (pair I) irreversibly decayed at 8.0 K. Furthermore, the lines at 8.0 K marked by "□" (pair II) decayed at 10 K, leaving another set of weak double quartet lines marked by "○" (pair III). Thus, three sets of double quartets, pairs I, II, and III, were separately observed. The spectra of the three different pairs consist of a constant isotropic hf value of 1.16 mT for the quartet, but of slightly different doublet splittings from 25.1 to 26.3 mT. The value of 1.16 mT (three equivalent H-atoms) is exactly one-half of that of the isolated CH_3 radicals (2.32 mT), and the value of ca. 26 mT is very close to one-half of that of the H-atoms trapped in the interstitial tetrahedral site and the interstitial octahedral site in the Ar crystal, 51.26 and 51.14 mT, respectively, after the second-order correction.[20,21] This clearly suggests that the observed double

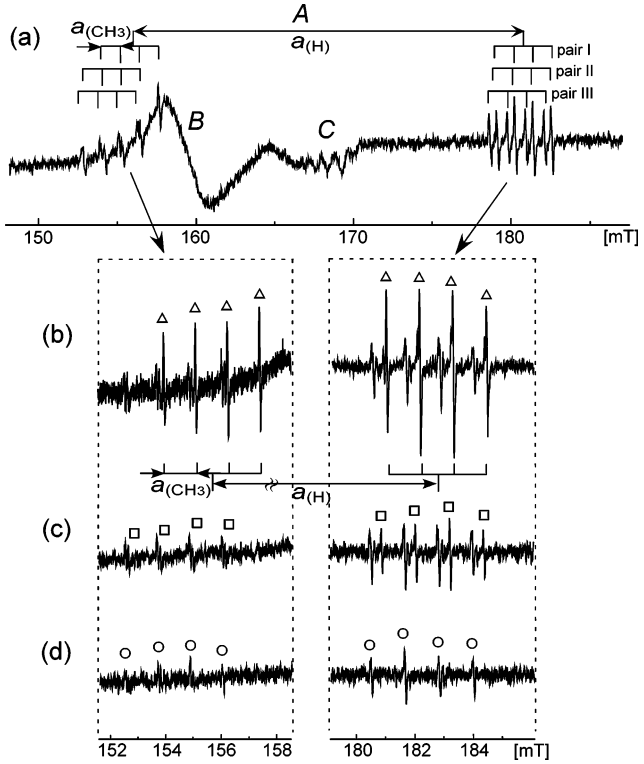

Figure 1. ESR spectra observed at $\Delta m_s = \pm 2$ transition for the CH_4 (0.05 mol %)/Ar system at (a) 4 K, (b) 5.8 K, (c) 8.0 K, and (d) 10 K for increasing temperature immediately after X-ray irradiation at 4 K. In spectra b−d, each band of the doublet separated by ca. 26 mT is expanded. The peaks due to three sets of pairs are marked by △, pair I; □, pair II; ○, pair III. The lines marked as A are attributable to the H···CH_3 radical pair. See text for the lines marked as B and C.

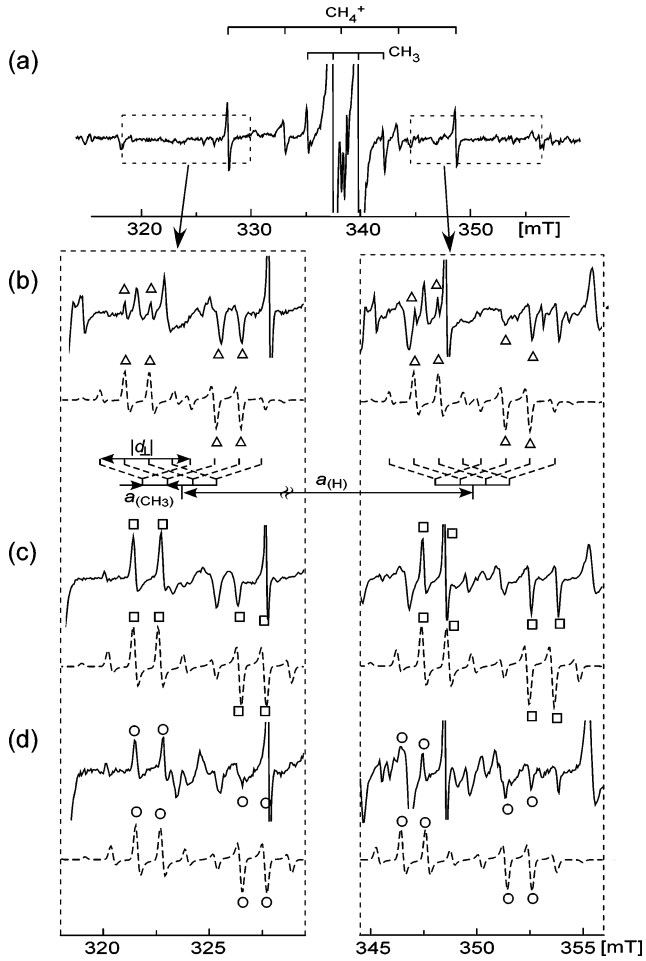

Figure 2. ESR spectra observed at $\Delta m_s = \pm 1$ transition for the CH_4 (0.05 mol %)/Ar system at (a) 4 K, (b) 5.8 K, (c) 8.0 K, and (d) 10 K for increasing temperature immediately after X-ray irradiation at 4 K. Spectra b−d are an expansion of $d_\perp$ components together with the corresponding theoretical line shapes (dashed line). The parameters used for the simulation are given in Table 1. The central two peaks ($m_I = \pm^1/_2$) due to three sets of pairs are marked by △, pair I; □, pair II; ○, pair III. The sample is the same as that in Figure 1.

quartets are attributable to the radical pairs of the H-atom with the methyl radical, H···CH_3. The radical pairs are expected to be in the triplet electronic ground state, which lies below the singlet state by 2*J* (the singlet triplet separation energy) with $|J| \gg a_{iso}$ of the isolated H-atom ∼1.4 GHz.[11] The ESR spectral resolution of the radical pair is quite high with a narrow line width of ca. 0.01 mT, which is much narrower than those of the previously reported radical pairs formed in the irradiated pure methane[5,6] and in rare gas matrices.[7−10] Because of the high resolution, three different sets of the double quartets could be separately observed, and the H-hf splittings at the $\Delta m_s = \pm 2$ transition could be evaluated with high accuracy.

As with the isolated CH_3 radical,[18] the quartet with the equal relative intensity (A_1-lines) was observed for the CH_3 radical in the H···CH_3 pair at the $\Delta m_s = \pm 2$ transition at 4 K as shown in Figure 1a. Moreover, the relative signal intensity for the radical pair is approaching the binomial one, 1:3:3:1, on increasing the temperature to 10 K in accord with the isolated CH_3 radical.[18]

3.2.2. Spectra at $\Delta m_s = \pm 1$ Transition. Figure 2 shows a spectrum at the allowed $\Delta m_s = \pm 1$ transition for the same CH_4/Ar sample as in Figure 1. In addition to the spectra due to the isolated H-atom, CH_3 radical, and CH_4^+ radical cation,[22] one can see the underlying complicated anisotropic spectra at 4 K. When the spectra were recorded with a higher amplitude gain and a high microwave power of 0.4 mW, the fs due to electron dipolar−dipolar coupling was clearly observed, accompanying the isotropic H-hf splittings.

By stepwise annealing the sample, the spectral lines irreversibly decayed out, and three different sets of H···CH_3 radical pairs, I (△), II (□), and III (○), were confirmed, similar to the case of the $\Delta m_s = \pm 2$ transition (Figure 1). The experimental spectrum is characterized by the anisotropic fs, in addition to an isotropic hf double quartet with ca. 26 and 1.16 mT splittings. The spectrum is symmetric with respect to the center, and only the perpendicular fs components ($d_\perp$) are visible here due to their much higher intensity than the parallel components ($d_\parallel$). In Figure 2b−d, the experimental spectra (solid lines) are compared to the theoretical ones (dotted lines) calculated with the following assumptions. We first assumed an axial symmetry for the fs principal values, $-d_\perp$ and $d_\parallel$, where $|-d_\perp| = d$. The *d* value is then assumed to be less than one-half of the isolated H-atom hf splitting (ca. 26 mT), but larger than one-half of the methyl H-hf splitting (1.16 mT). Under these conditions, the observed ESR spectra were successfully simulated for the randomly oriented H···CH_3 radical pairs using the H-hf splittings of the H-atom and the CH_3 radical and the *d* value as adjustable parameters with a constant line width of 0.2 mT having a Lorentzian type line shape.

The best-fit ESR parameters evaluated for radical pair I are $a_{iso} = 26.0$ and 1.16 mT for H-hf splittings of the H-atom and the CH_3 radical and $d = 4.2$ mT. Consistent with the results of the $\Delta m_s = \pm 2$ transition, the methyl H-hf splittings are 1.16 mT, remaining constant for the three radical pairs. However, the H-atom hf splittings slightly vary from 26.0 (for pair I) to

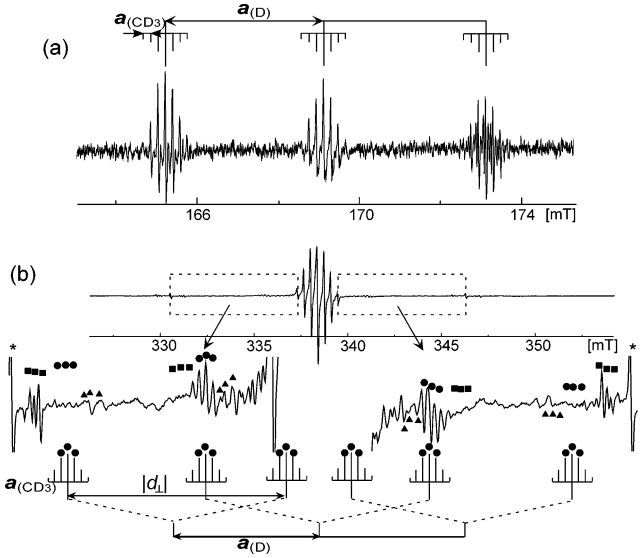

Figure 3. ESR spectra observed for CD_4 (0.01 mol %)/Ar at (a) $\Delta m_s = \pm 2$ transition and (b) $\Delta m_s = \pm 1$ at 4 K immediately after X-ray irradiation at 4 K. The expanded spectra in (b) show three different sets of pairs marked with ▲, pair I′; ■, pair II′; ●, pair III′. The stick diagram demonstrates for pair III′ how the $d_\perp$ components are further split by the $a_{(D)}$ and $a_{(CD_3)}$ hf splittings. The peaks due to the isolated D-atoms ($m_I = \pm 1$) are denoted by an asterisk (*). See text for details.

25.8 mT (for pair III). The most important point here is that the evaluated fs splittings are $d = 4.2$, 4.9, and 5.1 mT for pairs I, II, and III, respectively, suggesting a variety of trapping sites for the radical pair. The d values are very close to each other; however, the accompanying differences in g-factors and in H-hf splittings can help to extract each pair from the spectra with an uncertainty limit of less than ±0.1 mT.

3.3. D···CD_3 Radical Pairs in the CD_4/Ar System. It is of interest to investigate the deuterium isotope effects on the structure (i.e., hf splittings and fs pattern) of the radical pairs as well as on their yields. Thus, we examined the D···CD_3 radical pairs using CD_4 instead of CH_4 as the solute. The experimental spectra for the X-ray irradiated CD_4 (0.01 mol %)/Ar sample at 4 K are shown in Figure 3. Spectra a and b correspond to the forbidden $\Delta m_s = \pm 2$ and allowed $\Delta m_s = \pm 1$ transitions of the D···CD_3 radical pairs, respectively. The spectral pattern is more complicated than that of the H···CH_3 pair. Referring to the results for H···CH_3, however, we could successfully analyze the spectra as noted below.

The spectrum at $\Delta m_s = \pm 2$ consists of a triple septet with isotropic hf splittings of ca. 3.9 and 0.18 mT. The 3.9 mT splitting is one-half that of an isolated D-atom, 7.8 mT;[23] the D-atom hf splitting is reduced to 1/6.5 of the corresponding H-atom by the ratio of the nuclear magnetic moments of the H- and D-atoms, μ(D)/μ(H). The splitting of the septet, 0.18 mT, also corresponds to one-half that of an isolated CD_3 radical, 0.36 mT.[18] Thus, the pairwise trapping of the D-atom and the CD_3 radical is obvious for the irradiated CD_4/Ar system. In contrast to the H···CH_3 pair, the relative intensity of the septet is rather close to the binomial one (1:3:6:7:6:3:1). This can be explained in terms of easier thermal excitation to higher rotational levels with $J \geq 1$ for the CD_3 radical where the rotational constant is 2 times smaller than that of the CH_3 radical.[18]

In Figure 3a, we can see a septet clearly at the central band ($m_I = 0$) of the D-atom. At the $m_I = \pm 1$ bands, however, several sets of septets are overlapped. Upon increasing the temperature to 12 K, three sets of septet lines stepwise irreversibly disappeared at 7.8, 10, and 12 K. This allowed us to attribute the lines at the $m_I = \pm 1$ bands to three different sets of septets with slightly different D-atom hf splittings based on their thermal stability. In agreement with the results of the CH_4/Ar system, at least three different sets of the D···CD_3 radical pairs, I′, II′, and III′, were confirmed.

The anisotropic fs due to the D···CD_3 radical pairs became visible at the $\Delta m_s = \pm 1$ transition with spectrometer settings of a higher amplitude gain and a higher microwave power. Although the spectra are much more complicated than those of the H···CH_3 radical pairs, they were also successfully analyzed by referring to the results for the D···CD_3 pairs at the $\Delta m_s = \pm 2$ transition and those for the H···CH_3 pairs. The d values were evaluated to be 4.2, 6.5, and 5.9 mT for pairs I′ (▲), II′ (■), and III′ (●), respectively, by the spectral simulation method. The values are in the same range as but slightly greater than those of the H···CH_3 radical pairs (Table 1).

3.4. Radical Pairs in the CD_4−CH_4 (1:1)/Ar System. The ESR spectra observed for a solid Ar sample containing an equimolar mixture of CH_4 and CD_4 (0.25 mol % each) are shown in Figure 4. The spectra of two radical pairs, D···CD_3 and H···CH_3, in the triplet state are clearly observed at the $\Delta m_s = \pm 2$ transition. The d values and the H- and D-hf splittings were exactly the same as those for the D···CD_3 and H···CH_3 pairs formed in the mono-methane/Ar systems. If the radical pairs were statistically formed by the radiolysis, equal amounts of four different sets of the radical pairs, H···CH_3, H···CD_3, D···CH_3, and D···CD_3, should be observed. However, only two distinct pairs, H···CH_3 and D···CD_3, were observed in the CD_4−CH_4/Ar system; no trace of the other two radical pairs was observed. This result clearly demonstrates that the H-atom and the CH_3 radical (or the D-atom and the CD_3 radical) formed in pairs originate from the same methane molecule.

We observed a large H/D isotope effect on the yield of the radical pairs, [H···CH_3]/[D···CD_3]. The yield of the D···CD_3 pairs was about 15 times higher than that of the H···CH_3 pairs at 4 K based on the relative spectral intensity at $\Delta m_s = \pm 2$. The d-dependent transition probability[24] at $\Delta m_s = \pm 2$ was not taken into account in the estimate of the relative yield of radical pairs, H···CH_3 and D···CD_3, because the differences in d values between the two radical pairs are negligibly small as compared to the applied magnetic field strength (see Table 1). On the other hand, the yield of the isolated CD_3 radical was lower than that of the CH_3 radical, the ratio of yields, [CH_3]/[CD_3], being about 3 based on their signal intensity at $\Delta m_s = \pm 1$ at 25 K. This isotope effect on the relative yields is in contrast with that of the radical pairs as discussed in a later section (3.7. Reaction Scheme). Note that the 4 K ESR spectra of methyl radicals were saturated by applying a microwave power of 0.2 μW, which is a minimum value on the microwave bridge operated. To avoid the saturation, the relative yields of the methyl radicals were evaluated for the spectra at a higher temperature of 25 K where the signals were not saturated with 0.2 μW. It was confirmed that the relative yield of the methyl radicals was essentially independent of the measurement temperatures between 4 and 25 K. Furthermore, it should be noted that the total yield of the radical pairs was only about $^1/_{50}$ that of the methyl radicals.

3.5. H···CHD_2 and D···CH_2D Radical Pairs in the CH_2D_2/Ar System. When a partially deuterated methane, CH_2D_2, was used as the solute, the ESR spectra of two different radical pairs, H···CHD_2 and D···CH_2D, were observed as shown in Figure 5. No radical pairs of D···CHD_2 and H···CH_2D were observed. In agreement with the result of the CH_4−CD_4/Ar system, this observation suggests that the hydrogen atom and the methyl

TABLE 1: Experimental ESR Parameters of the Hydrogen−Methyl Radical Pairs and Probable Trapping Sites Proposed for the Counter Hydrogen Atom in Solid Ar Matrices

(a) H···CH_3 Radical Pairs

	$a_{(CH_3)}$/mT		$a_{(H)}$/mT				
H···CH_3	$\Delta m_s = \pm 1$	$\Delta m_s = \pm 2$	$\Delta m_s = \pm 1$	$\Delta m_s = \pm 2$	d/mT[a]	R[b]/nm	trapping site of H-atom (R/nm)[c]
pair I (△)	1.16	1.16	26.0	25.1	4.2	0.87	I_t (0.87) I_o (0.88)
pair II (□)	1.16	1.16	25.9	26.1	4.9	0.83	I_t (0.79) I_o (0.80)
pair III (○)	1.16	1.16	25.8	26.3	5.1	0.82	I_t (0.79) I_o (0.80)

(b) D···CD_3 Radical Pairs

	$a_{(CD_3)}$/mT		$a_{(D)}$/mT				
D···CD_3	$\Delta m_s = \pm 1$	$\Delta m_s = \pm 2$	$\Delta m_s = \pm 1$	$\Delta m_s = \pm 2$	d/mT[a]	R[b]/nm	trapping site of D-atom (R/nm)[c]
pair I′ (▲)	0.18	0.18	3.94	3.94	4.2	0.87	I_t (0.87) I_o (0.88)
pair II′ (■)	0.18	0.18	3.93	3.93	6.5	0.75	I_t (0.79) I_o (0.80)
pair III′ (●)	0.18	0.18	3.91	3.93	5.9	0.78	I_t (0.79) I_o (0.80)

[a] $d = |-d_\perp|$. d: fine structure parameter. $d_\perp$: the perpendicular component of the fine structure coupling tensor. [b] The inter-spin distance, R, was evaluated from the observed d value based on the point−dipole approximation. [c] It is assumed that the methyl radical occupies the substitutional site in the Ar crystalline fcc lattice and the counter H (D)-atom is in interstitial sites. See details in the text.

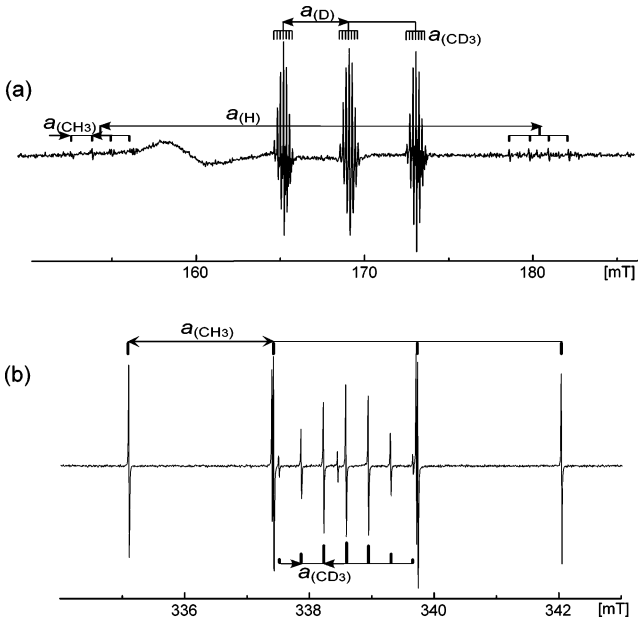

Figure 4. ESR spectra observed for the equimolar mixture of the CH_4−CD_4 (0.25 mol % each)/Ar system. (a) $\Delta m_s = \pm 2$ transition at 4 K immediately after X-ray irradiation at 4 K, (b) $\Delta m_s = \pm 1$ transition at 25 K for increasing temperature after X-ray irradiation.

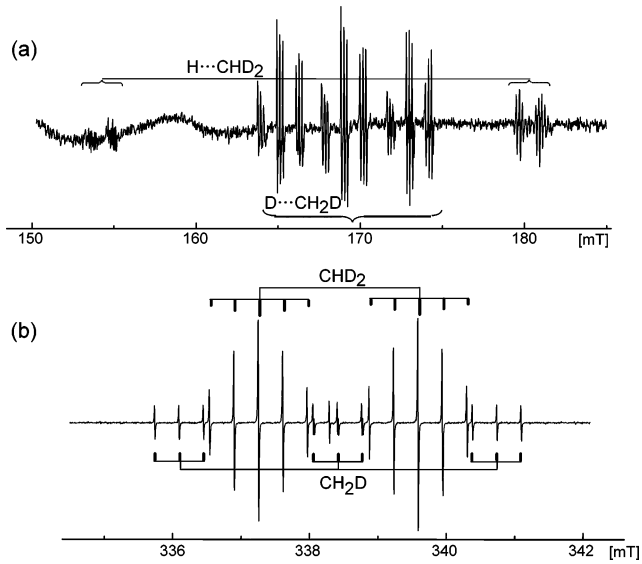

Figure 5. ESR spectra observed for the CH_2D_2 (0.5 mol %)/Ar system. (a) $\Delta m_s = \pm 2$ transition at 4 K immediately after X-ray irradiation at 4 K, (b) $\Delta m_s = \pm 1$ transition at 25 K for increasing temperature after X-ray irradiation.

radical as a pair come from the same CH_2D_2 molecule. Furthermore, a large H/D isotope effect on the radical yields was observed. The yield ratio of the radical pairs, [H···CHD_2]/[D···CH_2D], was ca. 0.2 at $\Delta m_s = \pm 2$ at 4 K, whereas that of the isolated methyl radicals, [CHD_2]/[CH_2D], was 8 at $\Delta m_s = \pm 1$ at 25 K. The observed isotope effect on the yield suggests that the H-atom is more difficult to dehydrogenate from CH_4 than the D-atom from CD_4 for the radical pair formation, but opposite for the isolated methyl radical formation.

3.6. Trapping Sites. The experimental H-hf splittings and d values are summarized in Table 1 for three different sets of each radical pair, H···CH_3 and D···CD_3, obtained from the $\Delta m_s = \pm 1$ and ± 2 spectra. Applying a point dipole approximation, the d value can be related to the separation distance between two radicals, R, by the following equation:[2,24]

$$d = (3/2)\mu_0 g\beta/4\pi R^3$$

where μ_0 is the magnetic moment of an electron (1.26×10^{-6} T^2 J^{-1} m^3), g is the g-factor of the radical (2.0022), and β is the Bohr magnetron for an electron (9.27×10^{-24} J T^{-1}). Replacing d by the experimental values of the H···CH_3 pairs, the distances are evaluated to be 0.87, 0.83, and 0.82 nm for pairs I, II, and III, respectively. Similarly, the R values for three sets of the D···CD_3 radical pairs are in the range from 0.75 to 0.87 nm, which are slightly smaller than those of the non-deuterated system.

On the basis of the ESR observations, we now discuss the trapping sites of the H-atom and the CH_3 radical formed in pairs

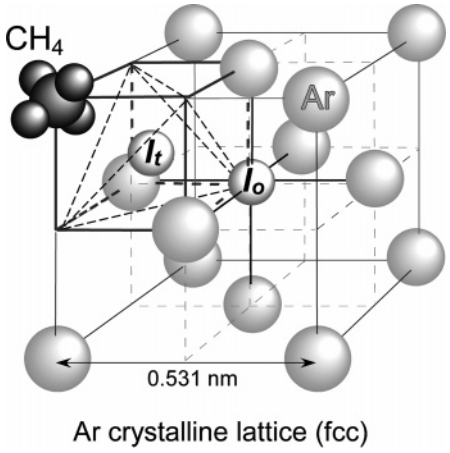

Figure 6. Schematic representation of trapping sites in an Ar crystalline lattice (fcc). A methane molecule is assumed to be in the substitutional site. One interstitial tetrahedral site (I_t) and one interstitial octahedral site (I_o) are indicated.[20]

in the Ar crystal. There are three possible trapping sites for the guest species: a substitutional (S) site, an interstitial octahedral (I_o) site, and an interstitial tetrahedral (I_t) site, in order of the void size, in the solid Ar crystal structure (fcc) with a lattice parameter of 0.531 nm (Figure 6).[20,25] The van der Waals volume of the CH_4 molecule is estimated to be 17.1 cm^3/mol, which is quite close to that of the Ar atom, 16.8 cm^3/mol.[19] It is reasonably assumed that one Ar atom is easily replaced by one methane molecule so as to occupy the S site. In this situation, the methyl radical formed by the C−H bond scission may retain the original S site of the mother molecule, without moving to other sites, taking its bulkiness and large mass into account. The validity of these assumptions can be supported by the fact that the H-hf splittings of the counter CH_3 radicals in three different sets of pairs are the same. Furthermore, the observed high-resolution spectra are consistent with the large void S site trapping due to the expected small interaction of the methyl radical with the surrounding Ar atoms.

In contrast to the CH_3 radicals, it is known that the hydrogen atoms, which are generated by the radiolysis of a hydrogen molecule in solid Ar at 4 K, occupy the I_t or I_o sites.[21] Thus, the most probable location of the counter H-atom is the I_t site directed away from the methyl radical being in the S site by a distance of 0.87 nm or the I_o site by a distance of 0.88 nm (Figure 7). These separation distances are very close to the experimental value, 0.87 nm, for the pair I (H···CH_3). For all other pairs, the I_t site or the I_o site, which produces the closest separation distance to the experimental value, were evaluated in a similar manner and summarized in Table 1.

3.7. Reaction Scheme. Most of the energy irradiated to the sample can be absorbed by the matrix Ar atoms due to the very low solute molecule concentrations of 0.01−0.5 mol %. In this case, the Ar atoms are expected to be ionized or excited or both (reaction 1) during the primary stage of radiolysis. There are two possible reaction mechanisms to explain the radical pair formation. One is a proton precursor mechanism associated with the ionization of the methane via the ionized Ar (Ar^+). The other is an excitation mechanism with the energy transfer to the methane via the electronically excited Ar (Ar*). In the former, a generated hole can be transferred from Ar^+ to the solute methane to form the methane radical cation, CH_4^+ (reaction 2), because of the lower ionization energy of the methane molecule than the Ar atom: $IP_1(Ar) = 15.76$ eV, $IP_1(CH_4) = 12.61$ eV.[26] In fact, we could observe the ESR spectrum of the CH_4^+ radical cation (Figure 2a). By interaction with

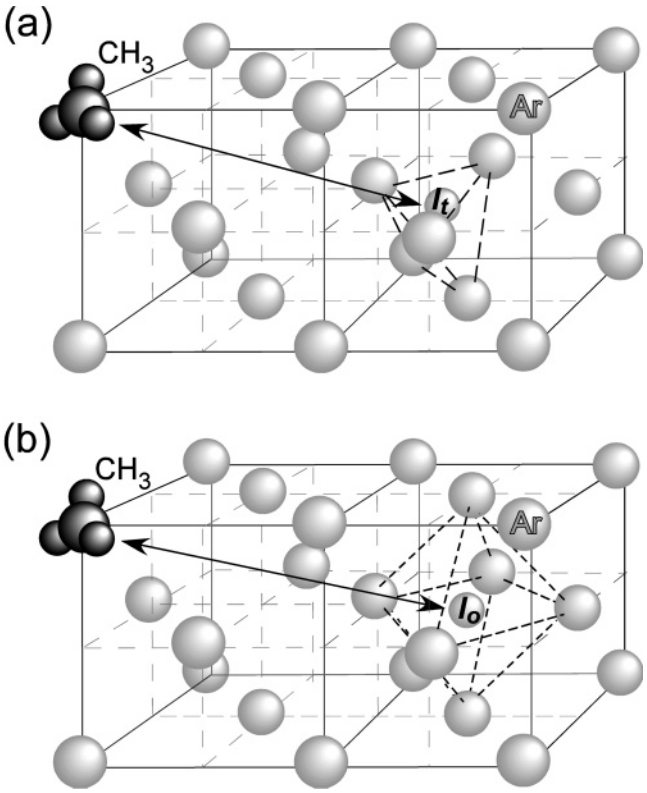

Figure 7. Schematics showing proposed trapping sites for the H···CH_3 radical pair with $d_\perp = 4.2$ mT (i.e., $R = 0.87$ nm) in solid Ar. The CH_3 radical occupies a substitutional (S) site in the Ar crystalline lattice (fcc). The counter H-atom occupies (a) the interstitial tetrahedral site, I_t, at a distance of 0.87 nm from the CH_3 radical, and (b) the interstitial octahedral site, I_o, at a distance of 0.88 nm. See text for details.

SCHEME 1

$$Ar \xrightarrow{\text{X-ray}} Ar^+ + e^-,\ Ar^* \quad \text{--- (1)}$$

$$Ar^+ + CH_4 \longrightarrow Ar + CH_4^+ \quad \text{--- (2)}$$

$$CH_4^+ \longrightarrow CH_3 + H^+ \quad \text{--- (3)}$$

$$H^+ + Ar_2 \longrightarrow Ar_2H^+ \quad \text{--- (4)}$$

$$Ar^* + CH_4 \longrightarrow Ar + CH_4^* \quad \text{--- (5)}$$

$$CH_4^+ + e^- \longrightarrow CH_4^* \quad \text{--- (6)}$$

$$CH_4^* \longrightarrow CH_3 + H \quad \text{--- (7)}$$

$$Ar_2H^+ + e^- \longrightarrow Ar_2H \quad \text{--- (8)}$$

surround Ar atoms, a proton (H^+) may then be easily detached from the CH_4^+ radical cation to form the CH_3 radical and Ar_nH^+ ($n = 1-3$) complexes (reactions 3 and 4 where $n = 2$). Assuming that the energetic relations in the gas-phase reactions could be retained in the solid Ar matrix at 4 K, reaction 4 might be rationalized by a large formation energy of the complex: for example, 467 kJ mol^{-1} (exothermic) for the Ar_2H^+ complex in the gas phase.[27] Following this reaction, the proton can capture an electron (reaction 8) to generate the H-atom, which is stabilized as the counter atom in the vicinity of the CH_3 radical to form the radical pair. In the latter mechanism, on the other hand, the excess energy is transferred to the methane molecule from the excited Ar atom to form an excited methane, CH_4* (reaction 5). The "hot" H-atom is then generated through the homolytic C−H bond scission of the CH_4* molecule (reaction 7).

In the present experiments, the radical pairs with an inter-spin distance less than 0.88 nm were observed. In the proton precursor mechanism, however, a wide distribution of the inter-spin distance greater than 0.88 nm could be expected on the basis of a possible higher mobility of H^+ (than H-atom) due to its physical nature of an elementary particle without an electron (or with a positive charge). It has been proposed that a proton could diffuse in solid rare-gas (Rg) matrices through "a ligand-switching reaction" (an exchange of one of the Rg ligands) via a tunneling effect, once the stretching vibrational mode of the tri-atomic molecule, Rg_2H^+, is excited.[28] Thus, the proton precursor mechanism may not be the case. The excitation mechanism then should be considered in the present system. Although we have no numerical data on the kinetic energy of the H-atom released from the excited methane molecule, it may be reasonable to expect that the H-atom has not enough kinetic energy to move a distance more than 1 nm away; the H-atom may be readily thermalized and trapped to form the radical pair coupled with the methyl radical. In an early contribution, the present authors reported an ESR study that any spectral change by the recombination reaction of the thermalized H-atoms, $H + H \rightarrow H_2$, could not be detected by cw-ESR in solid Ar matrices in the temperature range 4−13 K.[21] This suggests that there is little possibility of the H-atom abstraction reaction from the CH_4 molecule by the thermalized H-atoms. In contrast to this, it is reported that the mean displacement of the photolytically produced H-atoms, as a result of the 193 nm photolysis of HBr in xenon matrices, is on the order of 10 nm.[29] In the present system, however, all of the excess energy over the C−H bond dissociation energy cannot be dissipated into the translational degree of freedom of the atomic fragment, but the energy might be spent by the excitation of out-of-plane vibrational mode, ν_2 ($A_{2''}$), of the remaining CH_3 fragment. Hence, the excitation mechanism may be consistent with the present ESR results, showing a relatively narrow distribution of the inter-spin distance between 0.75 and 0.87 nm.

Comparing the yields of all of the radical products, the isolated methyl radical was almost 50 times greater than the radical pair; $[CH_3]/[H\cdots CH_3] \approx 50$. This result suggests that the formation reactions of the isolated radicals may be different from those of the radical pair; a proton precursor mechanism may be the major process to form the isolated radical species, H and CH_3, and an excitation mechanism is a minor one in the radiolysis of the solid Ar matrix at 4 K. Yoshida et al. measured the de-excitation cross sections of Ar* ($^3P_2$, $^3P_1$, $^3P_0$, and $^1P_1$) by the CH_4 in the gas phase and concluded that the ionization is not the predominant process, but the neutral fragmentation of the excited molecules predominantly follows from the energy-transfer processes from Ar*.[30,31] Their conclusion apparently conflicts with our proposition that the CH_4 ionization followed by the H^+ detachment may be the major process that forms the isolated CH_3 radical. The discrepancy, however, may come from the difference in reactions between the gas phase and the low-temperature solid phase.

Significantly large H/D isotope effects on the yield of the radical pairs were observed, when selectively deuterated methane or an equimolar mixture of methanes, CH_4-CD_4, was used as the solute. In the case of the equimolar mixture, for example, the yield ratio of $[D\cdots CD_3]/[H\cdots CH_3]$ was ca. 15. The following two explanations may be possible. One is the isotope effect on the C−H/C−D bonds scission via the excited methane molecule. The other is the isotope effect on the kinetic energy of the H- and D-atoms formed by the bond scission; the D-atom can be less mobile than H-atom due to its 2 times larger mass than the H-atom. No significant H/D isotope effects were, however, observed for the inter-spin distance of the radical pair. This suggests that the H/D isotope effects on the C−H/C−D bonds scission may be responsible for the observed isotope effects on the yield of the radical pairs. In further discussion of the reaction mechanism in detail, considerations including the zero-point energy differences should be taken into account.

4. Concluding Remarks

The high-resolution ESR spectra of spin exchanged radical pairs of the hydrogen atom coupled with the methyl radical, such as $H\cdots CH_3$, $H\cdots CHD_2$, $D\cdots CH_2D$, and $D\cdots CD_3$, were observed for the X-ray irradiated solid Ar matrices containing deuterium-labeled methanes at 4 K. The unique combination of the guest methane and the matrix Ar resulted in the high-resolution ESR observation of the radical pairs, as with the previous ESR study of the isolated methyl radicals,[18] but with the different spectrometer settings of higher microwave powers and higher gains.

The present high-resolution spectra allowed us to determine the accurate ESR hf and fs parameters, which made it possible to discuss the inter-spin distance, the trapping site, and the formation mechanism of the radical pairs. The spectra of the $H\cdots CH_3$ pairs for both the $\Delta m_s = \pm 1$ and the $\Delta m_s = \pm 2$ transitions consist of the double quartet lines with H-hf splittings of ca. 26 and 1.16 mT. For the $\Delta m_s = \pm 1$ transition, further splittings by the electron dipole−dipole interaction (fs parameter: d) were clearly observed, and the spectral line shapes were successfully simulated by the computations using the axial symmetric fs principal values, $-d_\perp$ and $d_\parallel$, where $|-d_\perp| = d$, as adjustable parameters. Because of the high-resolution with a narrow line width of ca. 0.01 mT ($\Delta m_s = \pm 2$) and 0.2 mT ($\Delta m_s = \pm 1$), three different sets of radical pairs were observed at 4.2 K, which were fairly well resolved in the spectra at both $\Delta m_s = \pm 1$ and ± 2 transitions by stepwise annealing the sample to 10 K. For the three different $H\cdots CH_3$ pairs, the fs parameters of $d = 4.2$, 4.9, and 5.1 mT were evaluated from the analysis of the anisotropic spectrum at the $\Delta m_s = \pm 1$ transition; the d values correspond to the respective inter-spin distances (R) of 0.87, 0.83, and 0.82 nm.

The H-atoms formed by the homolytic scission of the C−H bond may migrate in the Ar lattice (fcc) so as to be trapped in the interstitial tetrahedral (I_t) or octahedral (I_o) site, while the methyl radical may retain the substitutional site of the Ar crystal where the mother molecule originally occupied. Based on this assumption, the trapping sites of the counter hydrogen atom could be successfully attributed to each pair. For example, the I_t sites directed away from the methyl radical by a distance of 0.87 nm and/or the I_o sites by a distance of 0.88 nm are evaluated for the counter H-atom in pair I with $R = 0.87$ nm.

The present ESR study using the selectively deuterium-labeled methane, CH_2D_2 or the equimolar mixture of CH_4-CD_4, unambiguously revealed that the hydrogen atom and the methyl radical being in pairs originate from the same methane molecule. This result strongly suggests that the radical pair formation could be caused by the homolytic C−H bond scission via the electronically excited methane molecule (CH_4*). No trace of radical pairs other than the present three pairs was detected, suggesting that the H-atoms formed via CH_4* could not migrate distances greater than ca. 0.9 nm in the Ar matrix at 4 K. Significantly large H/D isotope effects were observed for the yield of the radical pair, but not for the separation distance. This is ascribed to the isotope effects on the C−H and C−D bond scission from CH_4* and CD_4*.

Acknowledgment. This work was partially supported by a Grant-in-Aid for Scientific Research (No. 17550178) from the Japan Society for the Promotion of Science, and by the Wenner-Gren Foundation (Sweden).

References and Notes

(1) Atkins, P. W.; Symons, M. C. R.; Trevalion, P. A. *Proc. Chem. Soc.* **1963**, 222.

(2) Kurita, Y. *J. Chem. Phys.* **1964**, *41*, 3926.

(3) Kurita, Y.; Kashiwagi, M. *J. Chem. Phys.* **1966**, *44*, 1727.

(4) Owen, J.; Harris, E. A. In *Electron Paramagnetic Resonance*; Geschwind, S., Ed.; Plenum Press: New York, 1972; p 427.

(5) (a) Gordy, W.; Morehouse, R. *Phys. Rev.* **1966**, *151*, 207. (b) Gordy, W. *Theory and Applications of Electron Spin Resonance*; John Wiley & Sons: New York, 1980.

(6) Toriyama, K.; Iwasaki, M.; Nunome, K. *J. Chem. Phys.* **1979**, *71*, 1698.

(7) Knight, L. B., Jr.; Rice, W. E.; Moore, L.; Davidson, E. R. *J. Chem. Phys.* **1995**, *103*, 5275.

(8) Van Zee, R. J.; Williams, A. P.; Weltner, W., Jr. *J. Phys. Chem. A* **1997**, *101*, 2917.

(9) Knight, L. B., Jr.; Rice, W. E.; Moore, L.; Davidson, E. R.; Dailey, R. S. *J. Chem. Phys.* **1998**, *109*, 1409.

(10) Knight, L. B., Jr.; Bell, B. A.; Cobranchi, D. P.; Davidson, E. R. *J. Chem. Phys.* **1999**, *111*, 3145.

(11) Shiotani, M.; Komaguchi, K. In *EPR of Free Radicals in Solids*; Lund, A., Shiotani, M., Eds.; Kluwer Academic: Dordrecht, 2003; p 153.

(12) (a) Kasai, P. H.; Whipple, E. B.; Weltner, W., Jr. *J. Chem. Phys.* **1966**, *44*, 2581. (b) Kasai, P. H. *Phys. Rev. Lett.* **1968**, *21*, 67. (c) Kasai, P. H.; Mcleod, D., Jr. *J. Am. Chem. Soc.* **1972**, *94*, 7975. (d) Kasai, P. H.; Himmell, H.-J. *J. Phys. Chem.* **2002**, *106*, 6765.

(13) (a) Knight, L. B., Jr.; Steadman, J.; Feller, D.; Davidson, E. R. *J. Am. Chem. Soc.* **1984**, *106*, 3700. (b) Knight, L. B., Jr.; King, G. M.; Petty, J. T.; Matsushita, M.; Momose, T.; Shida, T. *J. Chem. Phys.* **1995**, *103*, 3377.

(14) Shiotani, M. *Magn. Reson. Rev.* **1987**, *12*, 333.

(15) Andrew, L., Moskovits, M., Eds. *Chemistry and Physics of Matrix Isolated Species*; Elsevier: Amsterdam, 1989.

(16) Knight, L. B., Jr. In *Radical Ionic Systems*; Lund, A., Shiotani, M., Eds.; Kluwer Academic: Dordrecht, 1991; p 73.

(17) Kunttu, H.; Eloranta, J. In *EPR of Free Radicals in Solid*; Lund, A., Shiotani, M., Eds.; Kluwer Academic: Dordrecht, 2003; p 337.

(18) Yamada, T.; Komaguchi, K.; Shiotani, M.; Benetis, N. P.; Sørnes, A. R. *J. Phys. Chem. A* **1999**, *103*, 4823.

(19) Bondi, A. *J. Phys. Chem.* **1964**, *68*, 441.

(20) Foner, S. N.; Cochran, E. L.; Bowers, V. A.; Jen, C. K. *J. Chem. Phys.* **1960**, *32*, 963.

(21) (a) Komaguchi, K.; Kumada, T.; Aratono, Y.; Miyazaki, T. *Chem. Phys. Lett.* **1997**, *268*, 493. (b) Komaguchi, K.; Kumada, T.; Takayanagi, T.; Aratono, Y.; Shiotani, M.; Miyazaki, T. *Chem. Phys. Lett.* **1999**, *300*, 257.

(22) This is the first cw-ESR observation of the CH_4^+ radical cation isolated and stabilized in solid Ar matrix at 4 K.

(23) Jen, C. K.; Foner, S. N.; Cochran, E. L.; Bowers, V. A. *Phys. Rev.* **1958**, *112*, 1169.

(24) Atherton, N. M. *Electron Spin Resonance: Theory and Applications*; John Wiley & Sons: New York, 1973; p 150.

(25) Barret, C. S.; Meyer, L. *J. Chem. Phys.* **1964**, *41*, 1078.

(26) *CRC Handbook of Chemistry and Physics*, 83rd ed.; Lide, D. R., Ed.; CRC Press: Boca Raton, FL, 2002.

(27) Beyer, M.; Lammers, A.; Savchenko, E. V.; Niedner-Schatteburg, G.; Bondybey, V. E. *Phys. Chem. Chem. Phys.* **1999**, *1*, 2213.

(28) Beyer, M.; Savchenko, E. V.; N-Schatteburg, G.; Bondybey, V. E. *Low. Temp. Phys.* **1999**, *25*, 814.

(29) LaBrake, D.; Ryan, E. T.; Weitz, E. *J. Chem. Phys.* **199**5, *102*, 4112.

(30) Yoshida, H.; Kawamura, H.; Ukai, M.; Kouchi, N.; Hatano, Y. *J. Chem. Phys.* **1992**, *96*, 4372.

(31) Balamuta, J.; Golde, M. F.; Ho, Y.-S. *J. Chem. Phys.* **1983**, *79*, 2822.